

# CHERNOFF BOUND ON THE PROBABILITY OF ERROR FOR COMBINED LINEAR-DECISION FEEDBACK SEQUENCE ESTIMATION

Saeed A. Aldosari, Saleh A. Alshebeili and Abdulhameed M. Al-Sanie  
Department of Electrical Engineering  
King Saud University, P.O. Box 800, Riyadh 11421, Saudi Arabia

## Abstract

Decision feedback sequence estimation (DFSE) is a reduced state alternative to maximum likelihood sequence estimation (MLSE). One of the most popular techniques to improve the performance of DFSE is to process the received signal by a linear pre-filter prior to DFSE. This technique is referred to as combined-linear DFSE (CLDFSE). In this paper, we derive a tight upper bound on the error performance of CLDFSE. To the best of our knowledge, this bound is new and has not been yet considered in the literature. The simulation results show that the derived upper bound can be used to approximate the true BER performance of CLDFSE systems for a wide range of communication channels.

## 1 Introduction

Among techniques for combating intersymbol interference (ISI) in communication channels, Forney's maximum likelihood sequence estimation (MLSE) via Viterbi algorithm (VA)[1]. This technique has superior detection performance. However, the VA's computational complexity grows exponentially with the length of channel memory.

Decision feedback sequence estimation (DFSE) is a popular technique for reducing the complexity of the VA [2]-[3]. The DFSE technique is based on truncating the channel impulse response (CIR) in order to reduce the trellis searched by the VA. The DFSE algorithm is flexible in the sense that it allows a good tradeoff between complexity and performance, which ranges from the complex full VA to a simple DFE. However, the performance of DFSE highly depends on the structure of the channel under consideration. Specifically, DFSE is well suited for channels having most of their energy concentrated at the beginning of the CIR. For channels that does not satisfy this condition, such as nonminimum-phase channels, the performance of DFSE may become poor. This is because such channels tend to have a low minimum distance and high error propagation resulting from the decision feedback (DF) process inherent in DFSE [2].

Several authors have proposed using a linear pre-filter before the equalizer in order to shape the CIR into a one suitable for DF-based equalizers [4]. This

technique is referred to as combined-linear DFSE (CLDFSE).

Analytical solutions for the performance of digital communication systems are of great interest since they give more insight view of the factors governing the overall performance and the way they interact with each other. In this paper, we derive a tight upper bound on the error performance of CLDFSE. To the best of our knowledge, this bound is new and has not been yet considered in the literature. This bound can be used to develop a new criterion to improve designing the pre-filter of CLDFSE systems. Another advantage of the derived upper bound is that it can greatly simplify prediction of the BER of CLDFSE systems by using the bound as an approximator to the actual performance for medium to high SNR conditions. This is very essential especially when dealing with very low BER values at which conventional simulation techniques become impractical.

In the following section, we introduce the DFSE algorithm and discuss the factors affecting its performance. Second, we present the CLDFSE technique. Then, we derive a tight upper bound on the error performance of CLDFSE. Finally, we investigate the validity of implementing the derived bound as an approximator to the BER of CLDFSE system by comparing it with simulation results under different channel conditions.

## 2 The DFSE Algorithm

The DFSE is a technique for reducing the complexity of the VA based on truncating the states searched by the VA.

Consider a CIR  $\mathbf{h}$  of length  $L + 1$ . In DFSE, this channel is partitioned into two partitions by the parameter  $\ell$ , where  $0 \leq \ell \leq L$ . Hence, the DFSE states will consider only the last  $\ell + 1$  symbols while feeding back past decisions to eliminate residual ISI resulting from state truncation. Using this partitioning strategy, there are only  $M^\ell$  states instead of the  $M^L$  states required by the full complexity VA. Therefore, the complexity of DFSE can range from a simple DFE ( $\ell = 0$ ) to the full complexity VA ( $\ell = L$ ).

In DFSE, each state is defined by

$$t_k = [a_{k-1}, a_{k-2}, \dots, a_{k-\ell}], \quad (1)$$

and an error event occurs between times  $k_1$  and  $k_2$

if

$$\hat{t}_{k_1} = t_{k_1}, \hat{t}_{k_2} = t_{k_2}, \text{ but } \hat{t}_k \neq t_k \text{ for } k_1 < k < k_2 \quad (2)$$

where  $t_k$  and  $\hat{t}_k$  are the states of the correct and incorrect decoding paths at time  $k$ , respectively. The error vector  $e$  corresponding to this error event is defined as  $e = [\epsilon_{k_1}, \epsilon_{k_1+1}, \dots, \epsilon_{k_2-1}]$  and the components of  $e$  are defined as  $\epsilon_k = a_k - \hat{a}_k$ . The length of each error event is given by  $\Lambda = k_2 - k_1$ . We assume that the channel is stationary. Thus, the probability of an error event is independent of the start time of that error event and, hence, time 0 can be chosen as the start time without loss of generality [5]. The error event of length  $\Lambda$  can now be redefined as

$$e = [\epsilon_0, \epsilon_1, \dots, \epsilon_{\Lambda-1}]. \quad (3)$$

To evaluate the probability of occurrence of a particular error event we divide each error event into three subevents:

$E_1$ : at time 0,  $\hat{t}_0 = t_0$ ;

$E_2$ : the information symbols  $a_0, a_1, \dots, a_{\Lambda-1}$  when added to the error sequence  $\epsilon_0, \epsilon_1, \dots, \epsilon_{\Lambda-1}$  must result in an allowable sequence. In other words, the sequence  $\hat{a}_0, \hat{a}_1, \dots, \hat{a}_{\Lambda-1}$  must have valid values depending on the used modulation scheme;

$E_3$ : for  $0 \leq k \leq \Lambda - 1$ , the sum of the branch metrics of the estimated path exceeds the sum of the branch metrics of the correct path.

Given the above subevents, the probability of occurrence of a particular error event is bounded by [2]

$$\Pr(e) \leq \Pr(E_2) \Pr(E_3). \quad (4)$$

The probability of subevent  $E_2$  for  $M$ -ary PAM is given by [1]

$$\Pr(E_2) = \prod_{i=0}^{\Lambda-1} \frac{M - |\epsilon_i|/\delta}{M}. \quad (5)$$

The probability of subevent  $E_3$  is governed by the distance of the error event from the correct signal in the  $\Lambda$  dimensional space, which is called the Euclidean distance and is given by [2]

$$d_e = \sqrt{\sum_{k=0}^{\Lambda-1} \left( \sum_{i=0}^{\min(k,L)} h_i \epsilon_{k-i} \right)^2} \quad (6)$$

Since the noise is assumed to be a white Gaussian noise sequence with variance  $\sigma^2$ , the probability of subevent  $E_3$  is given by [2]

$$\Pr(E_3) = Q\left(\frac{d_e}{2\sigma}\right) \quad (7)$$

Substituting Equations 5 and 7 into 4 we get the upper bound on the probability of occurrence of error event  $e$  given by

$$\Pr(e) \leq Q\left(\frac{d_e}{2\sigma}\right) \prod_{i=0}^{\Lambda-1} \frac{M - |\epsilon_i|/\delta}{M}. \quad (8)$$

Summing up the probabilities of all possible error events multiplied by their Hamming weights we arrive to an upper bound of the overall symbol error probability given by

$$P_M \leq \sum_{e \in \mathcal{E}} \omega_e Q\left(\frac{d_e}{2\sigma}\right) \prod_{i=0}^{\Lambda-1} \frac{M - |\epsilon_i|/\delta}{M} \quad (9)$$

where  $\mathcal{E}$  denotes the complete set of valid error events and  $\omega_e$  is the number of nonzero components in each error event  $e$ .

### 3 Combined-Linear DFSE

From the last section, we note that the performance of DFSE is critically affected by the energy distribution of the CIR. Specifically, if there is a higher amount of energy concentration at the last coefficients of the CIR, two things may occur as a result of DFSE state truncation:

- the distance of error event, and consequently, the minimum distance may decrease considerably;
- error propagation due to the feedback process may increase significantly.

These two effects may cause severe degradation in the performance of DFSE when applied to such channels.

There are several techniques for improving the performance of DFSE. One of the most popular techniques is to process the received signal by a linear pre-filter prior to DFSE as shown in Figure 1. The aim of the pre-filter is to shape the original CIR into a one that has more energy concentration at the beginning of the impulse response to make it more suitable for DFSE. This technique is termed as *combined linear-DFSE* (CLDFSE).

The CLDFSE system as shown in Fig. 1 consists of a source that emits every  $T$  seconds an i.i.d zero-mean  $M$ -ary sequence  $\{a_k\}$ . The channel is modeled by a linear transversal filter  $\mathbf{h} = [h_0, h_1, \dots, h_L]$  and AWGN  $n_k$  of variance  $\sigma$ . The received signal is processed using a linear FIR filter  $\mathbf{w} = [w_0, w_1, \dots, w_N]$ . The output of the pre-filter given by

$$\begin{aligned} \mathbf{z} &= \mathbf{w} * \mathbf{y} \\ &= \mathbf{w} * \mathbf{h} * \mathbf{a} + \mathbf{w} * \mathbf{n} \end{aligned} \quad (10)$$

is then passed to the DFSE to produce the estimates  $\hat{a}_k$  of the transmitted sequence  $a_k$ . The DFSE is performed under the assumption that the desired impulse response (DIR)  $\mathbf{q}$  is of length  $\vartheta + 1$ . The DFSE operation is based on truncating  $\mathbf{q}$  to be of length  $\ell$ , where  $0 \leq \ell \leq \vartheta$ , while using feedback information extracted from the history of the survivor paths to eliminate part of the residual ISI resulting from state truncation.

It has been shown in [6] that introducing a delay parameter  $\Delta$  between the output of the DIR and the output of the pre-filter improves the performance of CLDFSE. Therefore, we can express the DIR  $\mathbf{q}$  in vector form as follows

$$\mathbf{q} = [g_\Delta, g_{\Delta+1}, \dots, g_{\Delta+\vartheta}]. \quad (11)$$

where  $g_k$  is the overall impulse response obtained by convolving the filter  $\mathbf{w}$  with the channel  $\mathbf{h}$ .

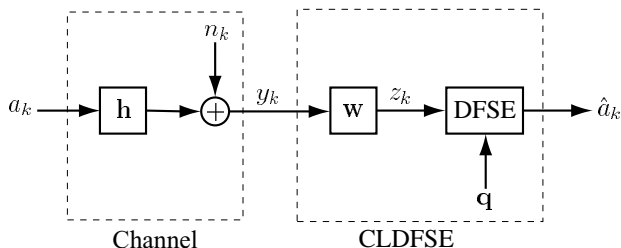


Figure 1: Combined linear-DFSE (CLDFSE).

## 4 Upper bound on the performance of CLDFSE

CLDFSE can be analyzed in the same way as the normal DFSE, i.e. by defining error events and analyzing their probability of occurrence. In DFSE, the noise component corrupting the input signal was assumed to be white and Gaussian, which simplifies the analysis of DFSE. On the other hand, when analyzing CLDFSE, one must consider the effect of two new factors, which are:

- noise correlations due to pre-filtering; and
- residual ISI resulting from truncation of the overall impulse response  $\mathbf{g}$  to one with a shorter extent  $\mathbf{q}$ .

Such factors complicate the analysis of CLDFSE as compared to DFSE. In what follows we derive a Chernoff bound on the probability of subevent  $E_3$ .

The model of the CLDFSE system in Equation 10 can be rewritten as

$$\mathbf{z} = \mathbf{a} * \mathbf{q} + \zeta \quad (12)$$

where  $\zeta$  represents the undesired term while  $\mathbf{a} * \mathbf{q}$  represents the desired one. The undesired term is composed of two components; the colored Gaussian noise  $\chi$  given by

$$\chi = \mathbf{w} * \mathbf{n} \quad (13)$$

and the untreated residual ISI  $\psi$  given by

$$\psi = \mathbf{b} * \mathbf{a} \quad (14)$$

where the coefficients of  $\mathbf{b}$  are given by  $b_k = g_k$  for  $k \notin \{\Delta, \Delta+1, \dots, \Delta+\vartheta\}$  and 0 otherwise. It can be

shown that the probability of subevent  $E_3$  is given by [7]

$$\Pr(E_3) = \Pr(\zeta_e \geq \frac{1}{2}d_e) \quad (15)$$

where  $\zeta_e$  is the projection of undesired term on the direction of the error signal  $\mathbf{u}$ . The error signal of an error event is given by

$$\mathbf{u} = [u_0, u_1, \dots, u_{\Lambda-1}]. \quad (16)$$

The elements of the vector  $\mathbf{u}$  can be determined using

$$u_k = \sum_{i=0}^{\Lambda-1} \epsilon_i q_{k-i} \quad \text{for } 0 \leq k \leq \Lambda-1 \quad (17)$$

and zero otherwise. Note that the length of the error signal  $\mathbf{u}$  of an error event  $e$  is nothing but the Euclidean distance of that error event  $d_e$ , i.e., we can define  $d_e$  as

$$d_e = \|\mathbf{u}\|. \quad (18)$$

The unit vector in the direction of the error signal is denoted by  $\mathbf{v}$  and is given by  $\mathbf{v} = \frac{\mathbf{u}}{\|\mathbf{u}\|}$ . The projections of the correlated noise  $\chi$  and the residual ISI  $\psi$  in the direction of an error event  $e$  are denoted by  $\chi_e$  and  $\psi_e$ , respectively, and are given by

$$\chi_e = \mathbf{v} * \chi \quad (19)$$

$$\psi_e = \mathbf{v} * \psi \quad (20)$$

Since the noise component  $\mathbf{n}$  introduced by the channel is assumed to be white and Gaussian, the corresponding noise  $\chi$  at the output of the linear pre-filter is also Gaussian but it is no longer white which means that its variance is not the same in all directions. From Equations 19 and 13 it can be shown that the correlated noise projection  $\chi_e$  has zero mean while its variance is given by

$$\sigma_{\chi_e}^2 = \sigma^2 \mathbf{v} \mathbf{C}_{\mathbf{w}\mathbf{w}} \mathbf{v}^T \quad (21)$$

Similarly, from Equations 20 and 14, it can be shown that the residual ISI projection  $\psi_e$  has zero mean (since the transmitted sequence is assumed to have zero mean) while its variance is given by

$$\sigma_{\psi_e}^2 = \sigma_a^2 \mathbf{v} \mathbf{C}_{\mathbf{b}\mathbf{b}} \mathbf{v}^T \quad (22)$$

where  $\sigma_a^2$  is the variance of the transmitted sequence. However, the residual ISI projection  $\psi_e$  is non-Gaussian and its distribution is unknown (but we know that its pdf has even symmetry since the input sequence is drawn from an even symmetric set). In the last two equations, the matrices  $\mathbf{C}_{\mathbf{w}\mathbf{w}}$  and  $\mathbf{C}_{\mathbf{b}\mathbf{b}}$  are  $\Lambda$  square matrices and their elements are given by

$$C_{\mathbf{w}\mathbf{w}}(i, j) = \sum_i \sum_j w_i w_{i-j}. \quad (23)$$

$$C_{\mathbf{b}\mathbf{b}}(i, j) = \sum_i \sum_j b_i b_{i-j}. \quad (24)$$

respectively.

To find the probability of subevent  $E_3$ , which is our main task, we need to evaluate the probability in Equation 15, i.e. we need to evaluate

$$\Pr(E_3) = \Pr(\chi_e + \psi_e \geq \frac{d_e}{2}). \quad (25)$$

However, since the distribution of  $\psi_e$  is unknown, it is difficult to evaluate Equation 25 exactly but we can find an upper bound.

It is clear that the pdf of  $\chi_e$  and  $\psi_e$  is even and, hence, the one-sided tail probability of Equation 25 can be replaced by the two-sided tail probability given by

$$\Pr(E_3) = \frac{1}{2} \Pr\left(|\chi_e + \psi_e| \geq \frac{d_e}{2}\right) \quad (26)$$

which can be expanded to the form [9]

$$\begin{aligned} \Pr(E_3) &= \frac{1}{2} \int_0^\infty \Pr(|\psi_e| \geq \tau) \left[ f_{\chi_e}\left(\frac{d_e}{2} - \tau\right) \right] d\tau \\ &\quad - \frac{1}{2} \int_0^\infty \Pr(|\psi_e| \geq \tau) \left[ f_{\chi_e}\left(\frac{d_e}{2} + \tau\right) \right] d\tau \\ &\quad + \frac{1}{2} \Pr\left(|\chi_e| \geq \frac{d_e}{2}\right) \end{aligned} \quad (27)$$

where  $f_{\chi_e}(\cdot)$  is the Gaussian pdf of  $\chi_e$  given by

$$f_{\chi_e}(x) = \frac{1}{\sqrt{2\pi\sigma_{\chi_e}^2}} \exp(-x^2/2\sigma_{\chi_e}^2) \quad (28)$$

and the variance  $\sigma_{\chi_e}^2$  has already been evaluated in Equation 21.

The only difficulty in Equation 27 is the evaluation of the two-sided tail probability  $\Pr(|\psi_e| \geq \tau)$  due to the unknown distribution of  $\psi_e$ . However, following the steps given in [10] we can write the Chernoff bound for this probability as

$$\Pr(|\psi_e| \geq \tau) \leq \begin{cases} 0 & \tau > \Psi \\ 2 \exp\left(-\frac{\tau^2\gamma}{4M\sigma_{\psi_e}^2}\right) & \Omega \leq \tau \leq \Psi \\ 1 & \tau < \Omega. \end{cases} \quad (29)$$

where

$$\Omega = \sqrt{\frac{4M\sigma_{\psi_e}^2 \ln(2)}{\gamma}} \quad (30)$$

$$\Psi = A \left( \sum_{i=0}^{L+N-2} |b_i| \right) \left( \sum_{i=0}^{\Lambda-1} |v_k| \right) \quad (31)$$

$$\gamma = \min_{k \geq 1} \left( \frac{(2k)!M}{k!} \right)^{1/k} \quad (32)$$

and  $A$  is the peak value of the zero-mean  $M$ -ary sequence  $\{a_k\}$ .

Finally, we substitute Equation 29 into 27 to get the upper bound on the probability of occurrence of subevent  $E_3$  given by

$$\begin{aligned} \Pr(E_3) &\leq \frac{1}{2} Q\left(\frac{d_e}{2\sigma_{\chi_e}}\right) \\ &\quad + \frac{1}{2} \int_0^\Omega \left[ f_{\chi_e}\left(\frac{d_e}{2} - \tau\right) - f_{\chi_e}\left(\frac{d_e}{2} + \tau\right) \right] d\tau \\ &\quad + \int_\Omega^\Psi \exp\left(-\frac{\tau^2\gamma}{4M\sigma_{\psi_e}^2}\right) f_{\chi_e}\left(\frac{d_e}{2} - \tau\right) d\tau \\ &\quad - \int_\Omega^\Psi \exp\left(-\frac{\tau^2\gamma}{4M\sigma_{\psi_e}^2}\right) f_{\chi_e}\left(\frac{d_e}{2} + \tau\right) d\tau \end{aligned} \quad (33)$$

By using the definition of the Q-function given by

$$Q(x) \triangleq \frac{1}{\sqrt{2\pi}\sigma} \int_x^\infty \exp(-y^2/2\sigma^2) dy. \quad (34)$$

we can minimize Equation 33 to get the bound

$$\begin{aligned} \Pr(E_3) &\leq \frac{1}{2} \left[ Q\left(\frac{d_e/2 - \Omega}{\sigma_{\chi_e}}\right) + Q\left(\frac{d_e/2 + \Omega}{\sigma_{\chi_e}}\right) \right] \\ &\quad + \beta \exp\left(\frac{\beta^2 - 1}{8\sigma_{\chi_e}^2} d_e^2\right) \left[ Q\left(\frac{\Omega/\beta - \beta d_e/2}{\sigma_{\chi_e}}\right) \right. \\ &\quad - Q\left(\frac{\Psi/\beta - \beta d_e/2}{\sigma_{\chi_e}}\right) - Q\left(\frac{\Omega/\beta + \beta d_e/2}{\sigma_{\chi_e}}\right) \\ &\quad \left. + Q\left(\frac{\Psi/\beta + \beta d_e/2}{\sigma_{\chi_e}}\right) \right] \end{aligned} \quad (35)$$

where

$$\beta = \frac{\sigma_{\psi_e}^2}{\sigma_{\psi_e}^2 + (\gamma/2M)\sigma_{\chi_e}^2} \quad (36)$$

Equation 35 represents an upper bound on the probability of subevent  $E_3$ . Knowing that the probabilities of the other two subevents  $E_1$  and  $E_2$  are similar to those of DFSE, we can find a bound on the overall symbol error probability  $P_M$  given by

$$P_M \leq \sum_{e \in \mathcal{E}} \omega_e \Pr(E_3) \prod_{i=0}^{\Lambda-1} \frac{M - |\epsilon_i|/\delta}{M} \quad (37)$$

where  $\omega_e$  is the number of nonzero elements in each error event  $e$  and  $\mathcal{E}$  is now defined as the set of all valid DFSE error events.

## 5 Simulation Results

In this section we investigate the validity of implementing the derived bound as an approximator to the BER of CLDFSE systems by comparing it with simulation results under different channel conditions. We have considered a BPSK i.i.d sequence transmitted through Channel-A, Channel-B, Channel-C and Channel-D with impulse responses shown in Fig. 2. A 50-tap linear pre-filter designed using the approach proposed in [8] was used to improve the overall performance of the 8-state CLDFSE system. In the simulation, we have used Monte Carlo runs to calculate the actual BER of the system.

It should be remembered that the CLDFSE performance bound presented in section 4 was derived

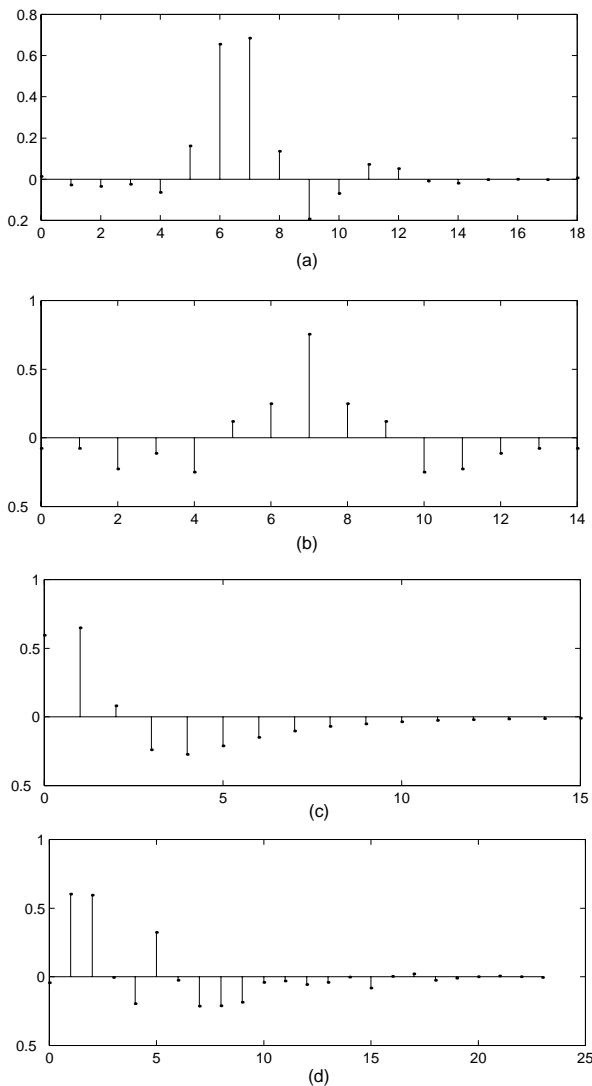


Figure 2: Channels impulse responses: (a) Channel-A, (b) Channel-B, (c) Channel-C, and (d) Channel-D.

assuming no error propagation. For this reason, we have also simulated the CLDFSE system under the assumption of no error propagation in order to compare it with its bound. This assumption can be implemented in the simulation program by insuring a separation of more than  $L - \ell$  correct decisions between any two adjacent error events [5].

Simulated and predicted BER values for all four channels are presented in Figures 3, 4, 5, and 6. From these plots, it can be seen that the predicted BER values using the derived upper bound closely matches the simulated results assuming no error propagation, especially for BER values that are below  $10^{-2}$ . Moreover, it can be seen that the simulated BER results assuming no error propagation approximately coincide with those when no assumptions are made for the cases of Channel-A, Channel-C and Channel-D, while they differ by about 0.25dB only for the case of Channel-B as can be seen from Figure 4. This clearly indicates that the effect of error

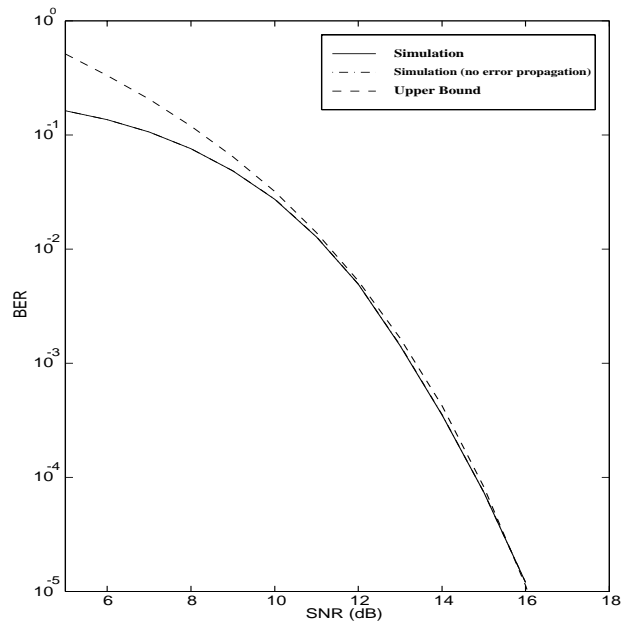


Figure 3: BER obtained from the derived bound and from the simulation for the case of channel-A.

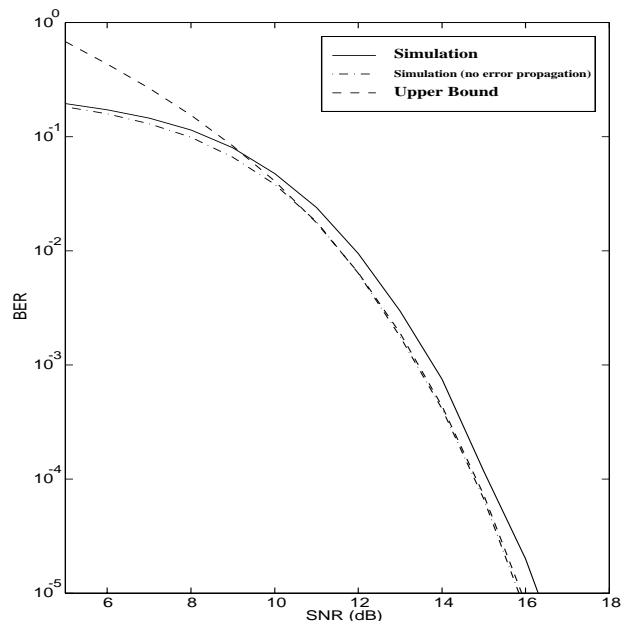


Figure 4: BER obtained from the derived bound and from the simulation for the case of channel-B.

propagation is small and usually can be neglected which means that the derived upper bound can be used to approximate the true BER performance of CLDFSE systems for a wide range of communication channels.

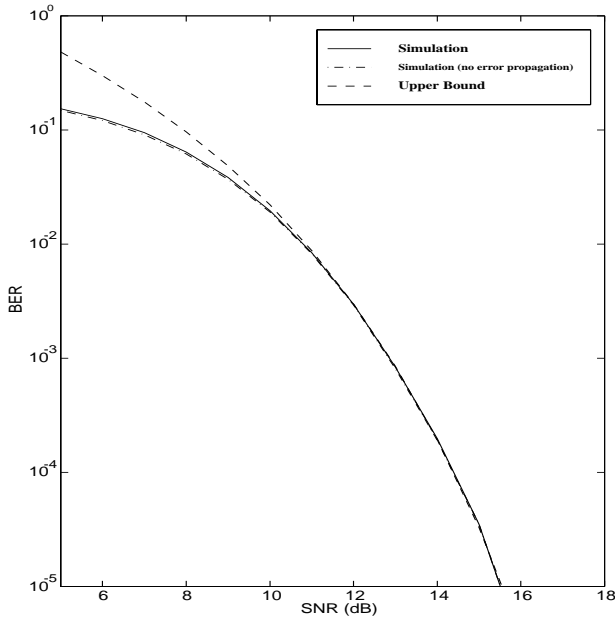


Figure 5: BER obtained from the derived bound and from the simulation for the case of channel-C.

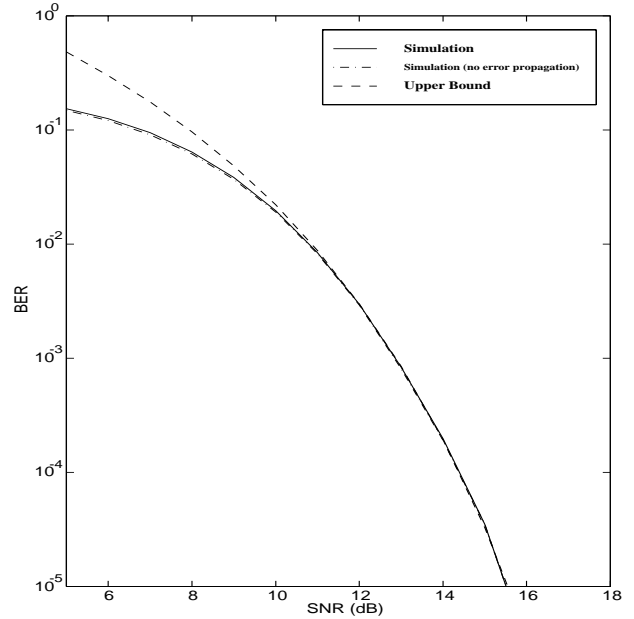


Figure 6: BER obtained from the derived bound and from the simulation for the case of channel-D.

## 6 Conclusion

In this paper, a tight upper bound on the error performance of CLDFSE has been derived. The simulation results have shown that the derived upper bound can be used to approximate the true BER performance of CLDFSE systems for a wide range of communication channels. Furthermore, this bound can be used to develop a new criterion to improve designing the pre-filter of CLDFSE systems.

## References

- [1] G. D. Forney, Jr., "Maximum-likelihood sequence estimation of digital sequences in the presence of intersymbol interference," *IEEE Trans. Inform. Theory*, vol. IT-18, no. 3, pp. 363-378, May 1972.
- [2] A. Duel and C. Heegard, "Delayed decision-feedback sequence estimation," *IEEE Trans. Commun.*, vol. 37, no. 5, pp. 428-436, May 1989.
- [3] M. Eyuboglu and S. U. H. Qureshi, "Reduced-state sequence estimation with set partitioning and decision feedback," *IEEE Trans. Commun.*, vol. 36, no. 1, pp. 13-20, January 1988.
- [4] J. G. Proakis, *Digital Communications*. McGraw-Hill, Singapore, second edition, 1989.
- [5] A. Hafeez, "Trellis and tree search algorithms for equalization and multiuser detection," Ph.D. Dissertation, The University of Michigan, 1999.
- [6] W. H. Gerstaecker and J. B. Huber, "Improved equalization for GSM mobile communications,"

in *Proc. Int. Conf. Telecommun.*, Istanbul, Turkey, pp. 128-131, April 1996.

- [7] S. U. H. Qureshi and E. E. Newhall, "An adaptive receiver for data transmission over time-dispersive channels," *IEEE Trans. Inform. Theory*, vol. IT-19, no. 4, pp. 448-457, July 1973.
- [8] S. A. Aldosari, S. A. Alshebeili and A. M. Al-Sanie, "Combined linear-decision feedback sequence estimation: an improved system design," submitted for *The IEEE international symposium in circuits and systems*, Sydney, May 2001.
- [9] R. Lugannani, "Intersymbol interference and probability of error in digital systems," *IEEE Trans. Inform. Theory*, vol. IT-15, no. 6, pp. 682-688, November 1969.
- [10] S. A. Aldosari, "Reduced complexity maximum likelihood sequence estimation for channels with intersymbol interference," M. Sc. thesis, King Saud University, May 2000.